NATIONAL RADIO ASTRONOMY OBSERVATORY
CHARLOTTESVILLE, VIRGINIA

ELECTRONICS DIVISION INTERNAL REPORT No. 256

A HIGH PERFORMANCE, 2.5 K CRYOSTAT INCORPORATING A 100-120 GHz DUAL POLARIZATION RECEIVER

JOHN W. ARCHER

DECEMBER 1984

NUMBER OF COPIES: 150

A HIGH PERFORMANCE, 2.5K CRYOSTAT INCORPORATING A 100-120 GHz DUAL POLARIZATION RECEIVER

John W. Archer

Table of Contents

Figures

Tables

Appendices

A HIGH PERFORMANCE, 2.5K CRYOSTAT INCORPORATING A 100-120 GHz DUAL POLARIZATION RECEIVER

John W. Archer

I. Introduction

For many applications in atmospheric physics and radio astronomy, the lowest possible receiver noise temperature is desirable. Furthermore, if the receiver is to operate at millimeter wavelengths and must be coherent, then cryogenically cooled systems of the heterodyne type must be employed. Until recently the best choice of the first mixer in such a receiver was a Schottky barrier diode device [1], [2]. The modern Schottky diode mixer has reached an advanced stage of development, may be easily and reliably cooled without performance degradation and exhibits low-noise temperatures and wide instantaneous bandwidth. Operation below about 20K results in little improvement in performance, allowing the use of reliable mechanical refrigerators.

A new mixer design, incorporating a superconductor-insulator-superconductor (SIS) junction, now challenges the status of the Schottky barrier diode device [3], [4]. SIS mixer receivers have achieved significantly lower noise temperatures than the best Schottky diode systems in the frequency range 100-230 GHz. In theory, mixers incorporating SIS devices are capable of noise temperatures approaching the quantum limit (4.8K at 100 GHz) and, with a correctly designed broadband mount, can also exhibit conversion gain [5]. The best SSB noise temperatures obtained with complete receivers are 80K at 115 GHz [6], 200K at 150 GHz [7], and 350K at 230 GHz [8]. The mixers used in these receivers all exhibited significant conversion loss. Mixers with conversion gain have been demonstrated at 110 GHz (T_{mxr}^{SSB} = 20K, G_{mxr}^{SSB} = +1.0 dB) [9] but have not as yet been incorporated into a receiver.

The superconductor junctions used in many SIS mixers are planar sandwich structures patterned photolithographically using lift-off techniques on lead alloy base and counter electrodes. Junctions with nominal areas of 5 μm^2 may readily by fabricated. To achieve with such junctions a sufficiently non-linear I-V response for efficient mixer performance requires that the device be cooled to below 3K. It is difficult to achieve this temperature simply and reliably using closed-cycle, mechanical refrigerators so batch cooling with liquid helium (He^4) is usually the preferred method of attaining satisfactory cryogenic operation [6].

The cryostat described in this paper was designed to incorporate two 100-120 GHz SIS mixers in a dual polarization receiver. Batch cooling with liquid helium is used, but the bath is surrounded by a radiation shield cooled to 20K using a mechanical refrigerator - the so-called "hybrid" cryostat [7], [10]. The paper describes how the cryogenic system was designed to be compact, holding only a maximum capacity of 4.3 liters of liquid, yet achieves exceptionally long liquid hold times at temperatures as low as 2.5K. The mixers used in the receiver were fabricated from a design by Pan et al. [6]; devices of this type have achieved the lowest reported noise temperatures in the 100-120 GHz band. Performance results for the NRAO version of these mixers in the new receiver cryostat are presented, which show that the single sideband receiver noise temperature is less than 120K between 100 and 120 GHz for both polarization channels.

II. Mechanical Description of the Cryostat

The position and orientation of the various components that make up the cryostat are best understood by reference to Figures 1, 2 and 3. Figure 1 shows a view of the interior of the top section of the dewar after the radiation shield covers have been removed. Figures 2 and 3 show cross sectional views through the complete dewar assembly along the planes indicated in Figure 1.

The 439.7 mm diameter x 254 mm high main vacuum vessel, made from 6061 aluminum, was fabricated in two cylindrical sections. The lower section is attached permanently only to the mechanical refrigerator head. To the top section are attached all the other components of the cryostat, including the radiation shields, the helium tank and the RF components. This allows easy dismantling of the system for maintenance by removal of the top dewar section only, and gives ready access to the mixers and backshort drive mechanisms. All demountable high vacuum seals in the system, such as between upper and lower dewar sections are made by BUNA-N rubber o-rings.

The refrigerator used to cool the radiation shields is a Cryogenics Technology, Inc. Model 1020. This two-stage, closed-cycle, helium refrigerant system operates using the Gifford-McMahon thermodynamic cycle to provide about 10W of cooling capacity at a secondary stage temperature of 20K and an additional 10W capacity at a primary stage temperature of 65K. The head is mounted on a cylindrical aluminum extension from the lower section of the main vacuum dewar, so that the face of the 20K mounting plate on the refrigerator is located 13 mm above the inside bottom wall of the dewar. An OFHC copper extension is bolted to the 65K flange of the refrigerator, providing a 65K mounting surface concentric with the 20K flange at a distance 6.65 mm above the internal dewar wall. As shown in Figures 2 and 3 the 20K and 65K radiation shields, attached to the

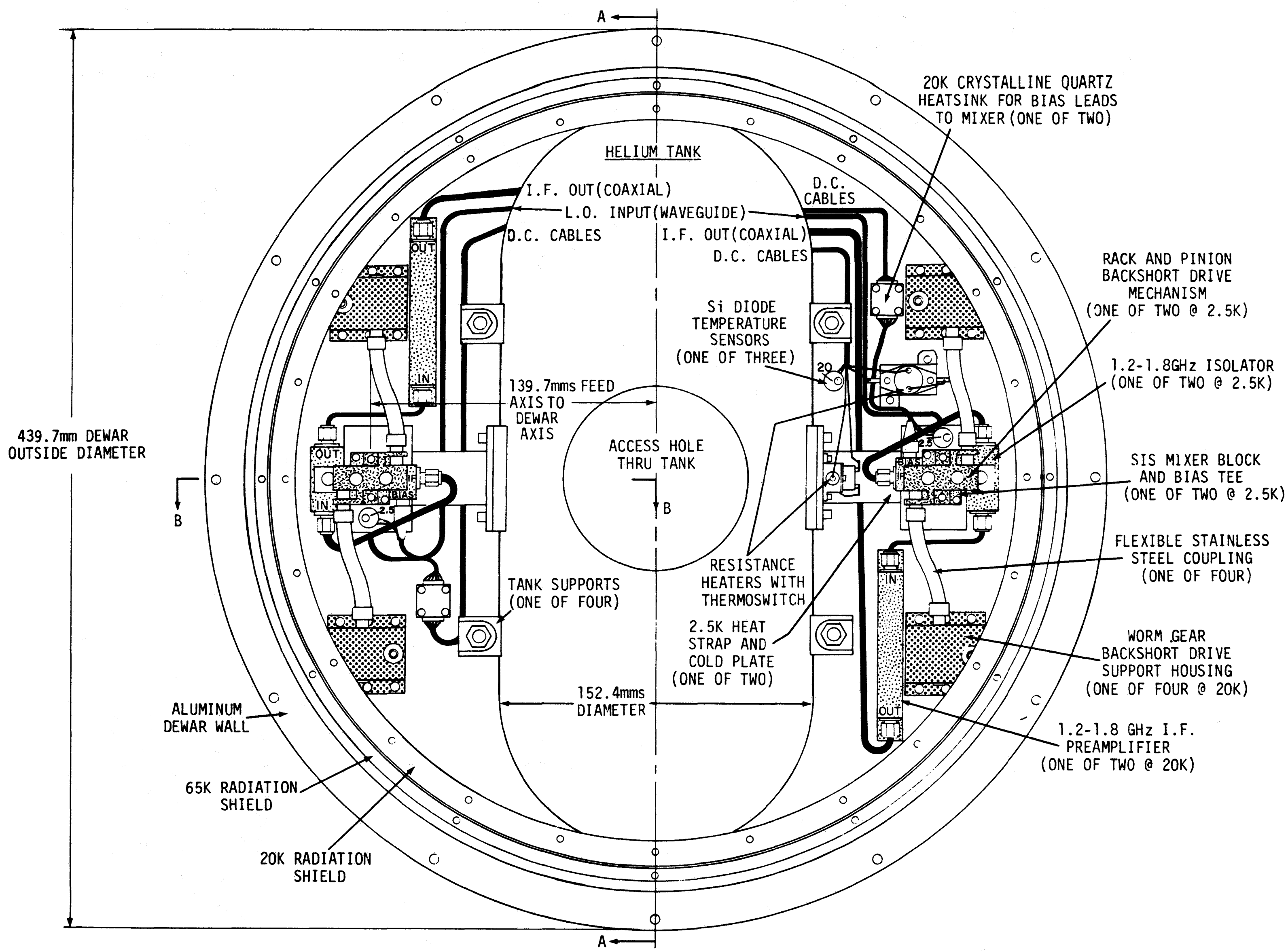

Fig. 1. A view of the interior of the top section of the vacuum dewar after the radiation shield covers have been removed.

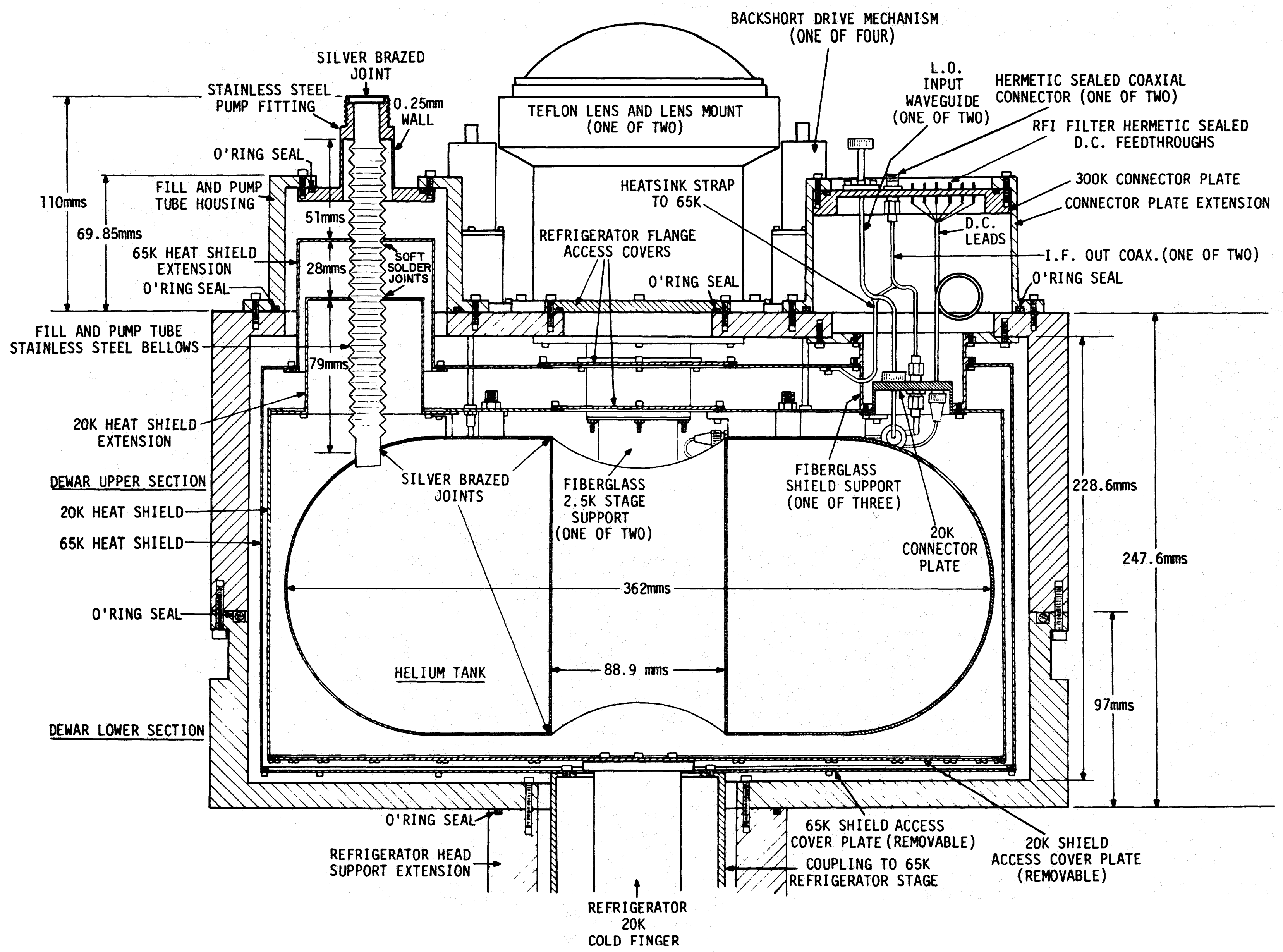

Fig. 2. Cross-sectional view of the complete dewar assembly along the diagonal AA shown in Figure 1. This sketch shows the tank mounting arrangement, heat shield locations and fill/pump tube configuration.

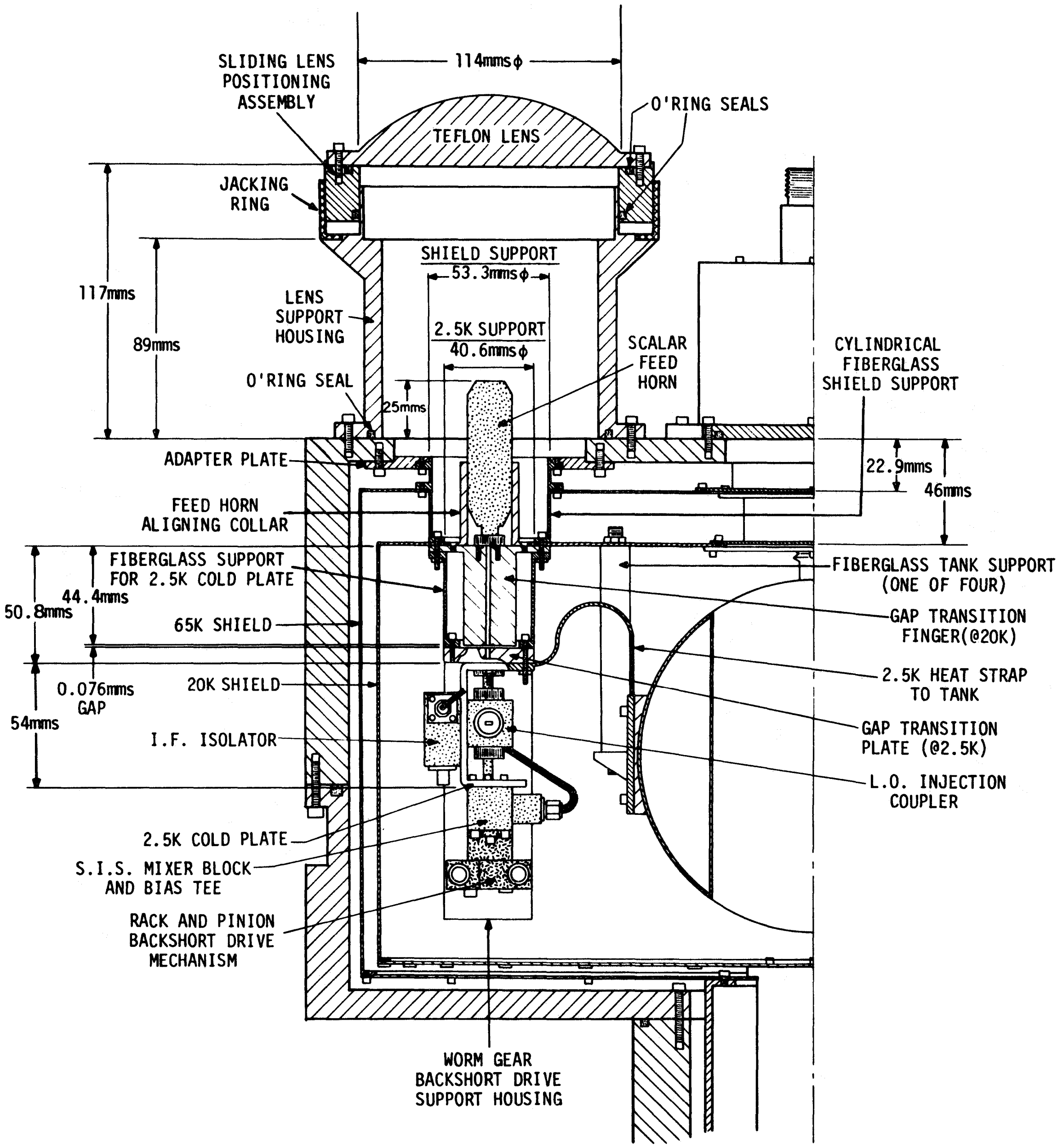

Fig. 3. Partial cross-section through one of the two R.F. assemblies, along the radius BB shown in Figure 1. Shown are the lens and feed horn geometry, the gap transition and the 2.5K cold plate to which the mixer is attached.

upper dewar section, bolt directly to these refrigerated flanges upon assembly of the two dewar halves.

The radiation shields were made from 0.635 mm thick sheets of OFHC copper rolled into cylindrical shapes around a mandrel. The lap joints and the joints between the end plate, the cover mounting ring and the cylindrical sections were made using a lead/tin alloy solder with 5% silver content. After fabrication the shields were brightly nickel plated to reduce their emissivity. Typical emissivities of the order of 0.15 were measured in a special test system for samples of this plated material. The inner (or 20K) shield, used to reduce radiative loading on the 2.5K components, has internal dimensions 178 mm deep x 376 mm diameter. The outer shield (at 65K), employed to minimize radiation loading on the 20K shield, has internal dimensions 205 mm deep x 389.5 mm diameter. Each shield has a removable, nickel-plated copper lower cover, which is held to the shield flange by a ring of bolts spaced at 15° intervals. The cover, in turn, attaches to the refrigerator flanges, thus transferring heat from the shield to the refrigerator.

If the 20K shield is to provide adequate thermal isolation for the 2.5K components, it is important that it be made completely opaque to infrared radiation. Holes in the shield wall have been kept to a minimum and those that are unavoidable have been appropriately baffled. A later section will further discuss the methods used for introducing and extracting DC and RF signals from the interior of the shield without radiation leakage.

The shields are attached to the wall of the upper dewar section at three points using cylindrical, thin wall, fiberglass standoffs (53.3 mm outside diameter x 1.27 mm wall), as shown in Figures 2 and 3. The fiberglass material has very low thermal conductance at cryogenic temperatures (2.4 mW/cm/K between 4 and

20K) and has a very good mechanical strength to weight ratio. The attachment between each shield and its supports is, however, not rigid. The special spacer arrangement shown in Figure 4 allows the shield to move radially relative to the support by about 0.5 mm, which is sufficient to relieve any stresses that might be set up by the shrinkage of the shield material upon cooling.

The liquid helium is contained in a cylindrical tank, which is completely enclosed and supported by the 20K radiation shield. The 4.3 liter capacity tank has an external diameter of 152.4 mm, a total length of 304.8 mm with hemispherical end-caps of 76.2 mm radius. An 88.9 mm internal diameter sleeve is inserted through the center of the tank, as shown in Figures 1 and 2, to allow access from above the dewar to the bolts which attach the radiation shields to the refrigerator flanges. In order to achieve a very uniform temperature distribution over its surface, the tank was made from OFHC copper by electroforming to a thickness of 0.76 mm over a hollow aluminum mandrel of the desired internal size. The hole to insert the sleeve was then bored through the copper and aluminum assembly and the aluminum etched away with a sodium hydroxide solution. The copper clearance sleeve was inserted, rolled over the tank at the seams and silver brazed in place. After brazing the fill/pump tube, the tank supporting brackets, and the flanges for connection of heat straps to cool RF components to the tank, it was brightly nickel plated on the exterior surface.

The tank is supported by four fiberglass cylinders (88.9 mm long x 12.7 mm outside diameter x 1.27 mm wall), which bolt at one end to brackets brazed to the tank and at the other end to the 20K shield. The fill and pumping tube for the tank is a seamless stainless steel bellows of 12.7 mm minimum internal diameter with a 0.15 mm wall and a total flex length of 152.4 mm. The bellows is heat sunk to the radiation shields at appropriate intervals by soldering

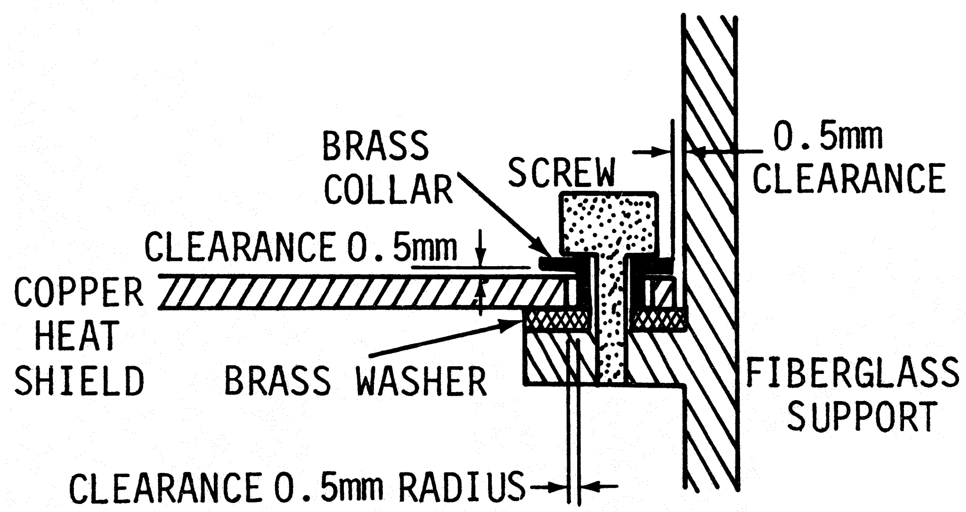

Fig. 4. A sketch illustrating the manner in which the heat shields are mounted, allowing for movement due to shrinkage during cooldown.

to cylindrical extensions made from OFHC copper, which are fixed to the respective shields with bolts. Apart from providing thermal isolation between the 2.5K, 20K and 65K stages and vacuum isolation between dewar and tank, the flexible bellows also allows movement between the tank, the shields and the dewar wall. At the outer dewar wall, the bellows is silver brazed to a stainless steel flange which incorporates a threaded fitting to allow a vacuum pumping, gauging and valving fixture to be attached. A thin wall section is incorporated in this flange (0.25 mm wall x 2.54 mm outside diameter) in order to thermally isolate the pumping fixture from the o-ring which seals the flange to the main dewar extension housing. This avoids problems with freezing of the rubber o-ring and consequent loss of vacuum in the main dewar when the cold outflowing helium gas from the tank cools the bellows and attached fixture. The measured helium leak rate for the complete tank and bellows assembly was less than 10^{-9} std. cc./sec.

Because of the mechanical design of the external flange and the shield extensions, removal of the tank is straightforward and requires only a few minutes. First, the bolts holding the dewar extension housing and the stainless steel flange to each other and to the dewar wall are removed. This permits access, from the outside of the vacuum vessel, to the screws which hold the first shield extension to the 65K shield. Then, from the inside of the 20K shield, a special screwdriver is used to remove the bolts which hold the 20K shield extension in place. Upon removing the four nuts holding the tank to the fiberglass supports and disconnecting the heat straps to the RF components, the tank may be easily lifted out of the interior of the 20K shield.

III. Configuration and Location of the Receiver RF Components

A block diagram of the receiver electronics is shown in Figure 5. Two SIS mixer blocks are mounted symmetrically on either side of the centrally located helium tank, as shown in Figure 1. Each mixer is screwed to a copper bracket which is supported by a cylindrical fiberglass standoff (40.6 mm diameter x 0.635 mm wall x 41.55 mm long) mounted concentrically with two diagonally opposite 20K heat shield supports. In order to cool the RF components with little temperature difference between the helium bath and the mixer, the bracket extends as one piece to the flange on the tank, thus minimizing the thermal resistance of the connection. The section of the bracket forming the heat strap between tank and support is thinned and bent in an S shape to relieve the stress that might occur as the materials at either end shrink differentially on cooling.

The bracket supporting and heat sinking each mixer also holds and cools a cross guide 20 dB coupler in WR-8 waveguide, used for local oscillator injection, and a 1.3-1.7 GHz isolator in the IF circuit, connected, as shown in Figure 5, between mixer and IF amplifier. Each 1.2-1.8 GHz GaAs FET IF amplifier [11] is mounted on the 20K shield and connected to the isolator at 2.5K via a 15 cm length of 2.13 mm diameter, 50 ohm, beryllium copper (inner and outer) coaxial cable, which provides good thermal isolation and acceptably low signal loss.

The cylindrical fiberglass standoffs that support each 2.5K cold plate also serve, as shown in Figure 3, to precisely locate the components of a gap transition, which couples the input signal from the scalar feed horn, cooled to 20K, to the mixer and LO coupler at 2.5K. The WR-8 waveguide transition, with a 0.076 mm gap between the input (at 20K) and output (at 2.5K), has measured insertion loss of less than 0.02 dB between 100 and 120 GHz and provides excellent thermal isolation. In addition, with the feed horn at 20K using such a transition,

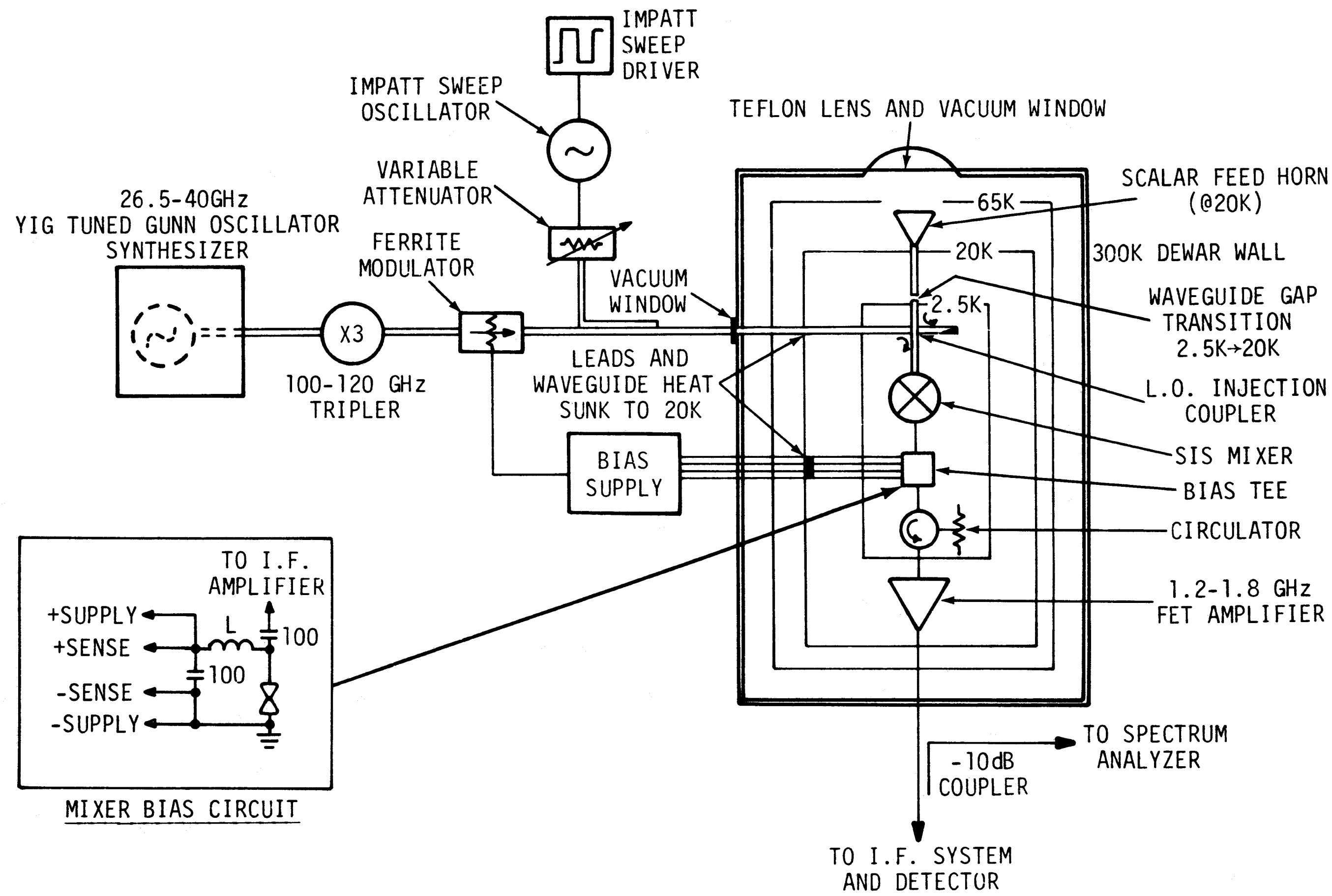

Fig. 5. A block diagram of one channel of the dual polarization receiver, showing the major R.F. components. The inductance L in the bias T is a coil wound on a miniature ferrite toroid. It is self resonant at 1.5 GHz. The capacitors are low inductance chips.

the need for a large window in the 20K shield that would occur if the feed were cooled to 2.5K is eliminated; so are consequent problems with inward leakage of infrared radiation or extraneous loss in the RF signal path. The pair of choke grooves for the transition are machined into the face of the 20K finger, concentric with the axis of the 2.03 mm x 1.02 mm waveguide. The grooves are 0.36 mm wide x 0.64 mm deep with inside diameters of 2.34 mm and 3.66 mm. When cooled to 20K, the fiberglass outer support and inner copper finger exhibit a change in length equal to within 10%, the fiberglass shrinking slightly more than the copper. Hence, the gap is reduced by only 10% from its room temperature setting (0.084 mm) upon cooling.

Figures 6 and 7 illustrate the mixer backshort drive mechanism. Since the mixers require two independent backshort adjustments, provision must be made for four separate drives external to the dewar. In addition, the drive mechanisms must be designed so that they are integral with the top dewar section and do not have to be dismantled to remove the mixers. As shown in Figure 7, rack and pinion mechanisms are used on the mixers to translate the linear motion of each short to a rotary motion about an axis at right angles to the direction of short translation. The linear displacement is a very sensitive function of angular rotation (3.175 mm/rad) so reduction gearing is essential between the external drive and the pinion shaft. Reduction and re-orientation of the input drive shaft are accomplished using a worm and worm wheel, as shown in Figure 6, with a 60:1 reduction ratio. The rack and pinion assembly (at 2.5K) on each mixer is connected to the worm wheel shaft (at 20K) by a flexible stainless steel bellows (6.33 mm inside diameter x 0.15 mm wall x 50 mm long) which provides good thermal isolation and axial flexibility, but has excellent rotational rigidity.

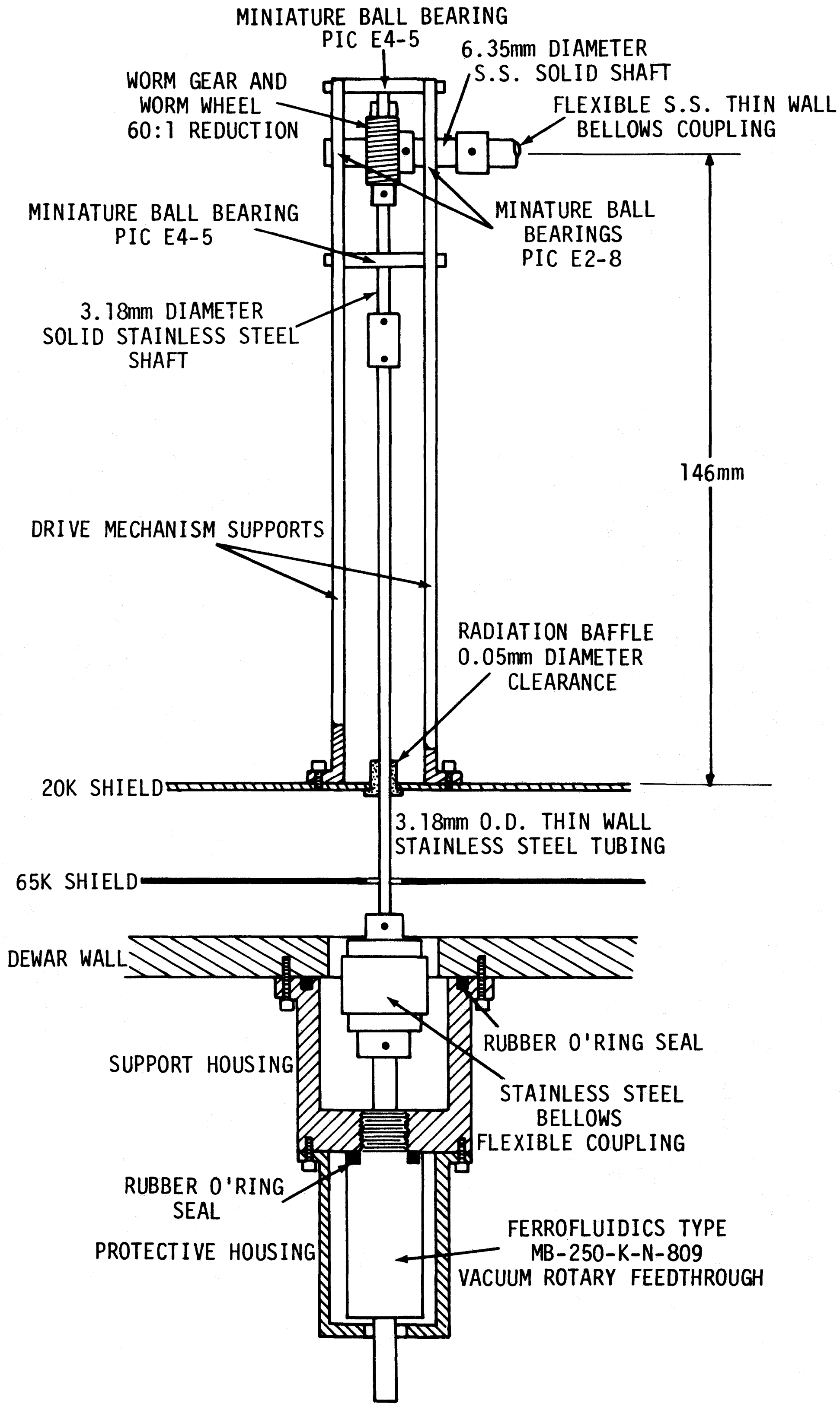

Fig. 6. A sketch illustrating one of the backshort drive mechanisms in the receiver dewar. Four identical units are installed in the positions shown in Figure 1.

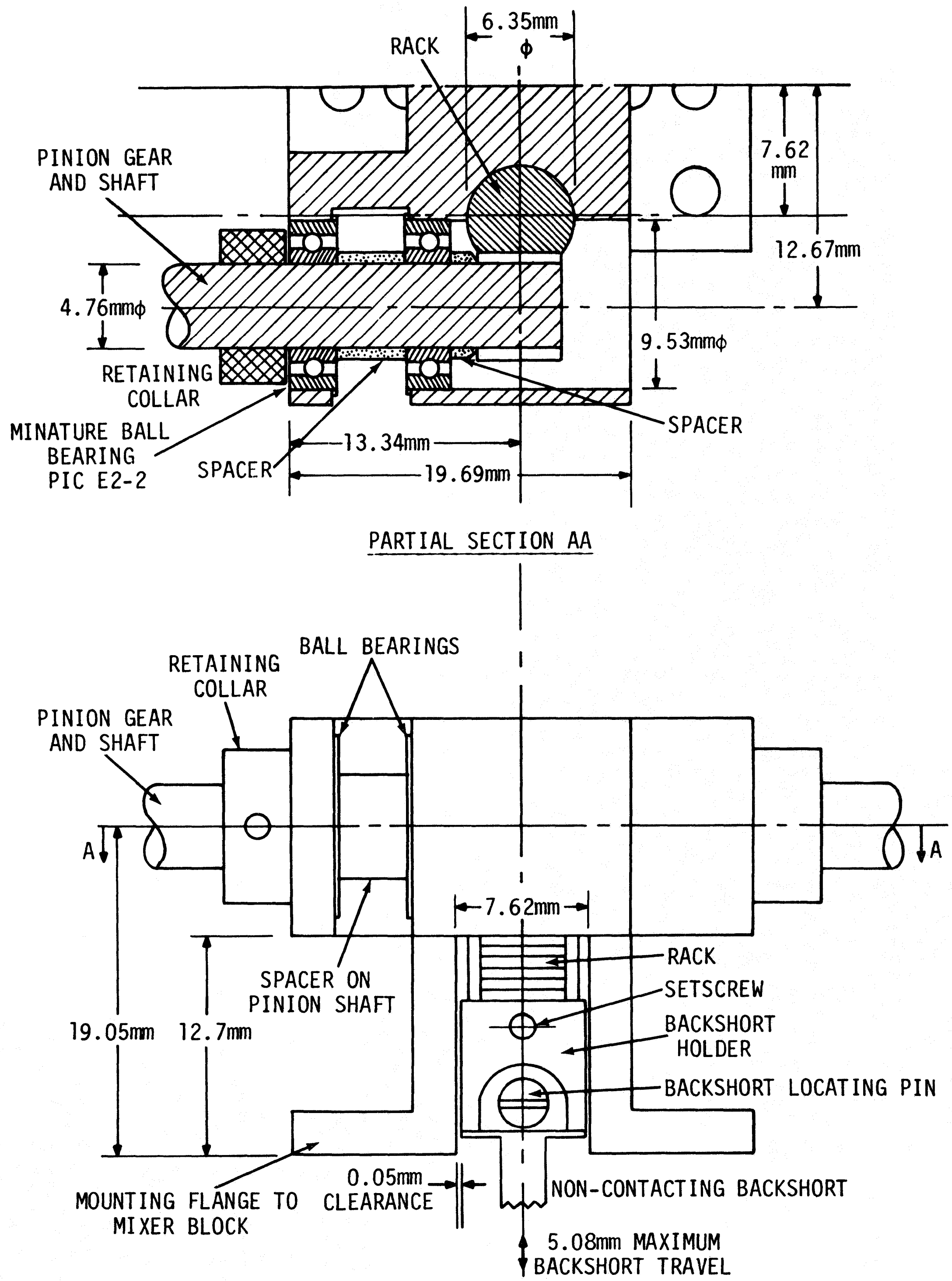

Fig. 7. **The rack and pinion mechanism installed on each mixer. This system converts the linear motion of each backshort to a rotary motion compatible with the drive mechanism shown in Figure 6.**

The final drive sensitivity is 0.053 mm/rad which is quite acceptable for 100 GHz mixer tuning. Backlash is less than 1/4 turn for the complete mechanism.

At the external wall of the dewar, a Ferrofluidics, type MB-250-K-N-809, rotary vacuum feedthrough is used, as shown in Figure 6, to transfer the drive motion to the inside of the cryostat. This shaft drives a commercial stainless steel bellows coupling which takes up axial and lateral motion due to differential contraction when the 20K shield is cooled. The rotary motion is then coupled to the worm gear using a 3.13 mm diameter x 0.25 mm wall stainless steel tube, which passes through a radiation baffle with 0.05 mm clearance in the wall of the 20K shield.

The orthogonally polarized radiation beams from the telescope optics are incident on the receiver axis and must be split spatially and the polarizations re-oriented before being input to the two separate receiver channels. A simple, very low loss, quasi-optical polarization splitter, which has been described previously elsewhere [12], is used to separate the orthogonally polarized components of the beam and direct the resulting pair of beams into the physically separated channels. The polarizer also rotates the polarization of one of the output beams through 90° so that the polarizations at both inputs to the dewar are parallel, thus simplifying mixer mounting. The incoming radiation in each channel is focused into a scalar feed horn in the dewar by a groove matched lens made from Teflon, which also serves as a vacuum tight RF window to the dewar. The design of both the lens and the feed horn are identical to a design described in a previous paper [12] and will not be detailed here except to state that the feed/lens combination has a far field beamwidth at the -11 dB points of 4.2°, independent of frequency between 100 and 120 GHz and introduces a total loss in the RF path of less than 0.15 dB over the same frequency range.

DC monitoring signals, such as from diode temperature sensors, DC bias inputs for the mixers and amplifiers, the IF output signals and the LO input power are all brought to and from the receiver via a common port, located diagonally opposite the tank fill/pump fixture. A flange on the exterior of the dewar, shown in Figure 2, incorporates special mountings for two WR-8 waveguide vacuum windows, two hermetically sealed SMA connectors and fifty hermetically sealed RFI filter feedthroughs for DC leads. Thin wall (0.25 mm wall) stainless steel waveguide brings the LO signals to a second special flange bolted to the 20K shield, which incorporates low radiation leakage feedthroughs for RF, IF and DC signals. The IF signals are carried from this flange using 2.13 mm outside diameter beryllium copper coaxial cable. Both waveguide and coax are heat sunk halfway along their length to 65K via a copper braid attached to the 65K shield, thus reducing the conductive heat load on the 20K shield. The coax and waveguide are also bent in an S shape between the two anchoring points to relieve possible stress buildup due to differential shrinkage upon cooling. Inside the 20K shield, the stainless steel waveguide is continued to bring the LO signals to the directional couplers at 2.5K. Since the required LO power is low for an SIS receiver, the loss in the LO waveguide runs is not an important parameter and so unplated guide was used with its higher thermal resistance.

All DC connections between 300K and 20K are made using #26 AWG enamelled bifilar brass wire, which has acceptably low electrical resistance but high thermal resistance. Leads which continue from 20K to 2.5K, such as for temperature sensors and mixer bias connections, are efficiently thermally coupled to the 20K shield using a special crystalline quartz heatsink. The heatsink consists of a 0.029 mm thick piece of gold metallized crystalline quartz (a very good heat conductor at 20K) epoxied to a copper carrier, which is bolted to the 20K shield. Six parallel gold paths, along which the DC signals pass, are etched onto the exposed surface of the metallized quartz, thus efficiently thermally coupling the leads to 20K. Miniature connectors are used at the input and output of the heatsink, making the arrangement easy to disconnect and remove.

IV. Vacuum System and Cooldown Procedures

Figure 8 illustrates the rather complex vacuum pumping and control system used with the hybrid cryostat. The main reason for the complexity is to minimize the chance of a loss of vacuum in either main dewar or tank during operation, with a consequent catastrophic vaporization of the liquid helium or the formation of an ice plug in the pump tube. The primary vacuum source is a mechanical vacuum pump made by Marvac, Inc. It is used both for roughing out the main dewar vacuum space and for pumping on the liquid helium bath. Both vacuum systems are protected against pump failure by solenoid operated, normally closed valves, which failsafe to the closed position upon loss of AC power to the pump or significant deterioration in pumping efficiency.

For the main dewar, a second manually operated, bellows sealed valve leads to the main vacuum chamber. This valve incorporates a locking device to protect against accidental opening. Permanently connected to the main dewar chamber are a cold cathode vacuum gauge (10^{-3} - 10^{-8} torr) and, through a secondary butterfly valve, a high vacuum Vac Ion pump. In normal operation, before starting to cool the radiation shields, the dewar vacuum space would be rough pumped to $< 10^{-2}$ torr and then pumped to 10^{-5} torr using the Vac Ion pump. A vacuum of this quality reduces the conductive loading through the residual gas and hence the initial cooldown time for the large surface area shields. With the shields cold and efficiently cryo-pumping, vacuum of the order of 10^{-7} torr

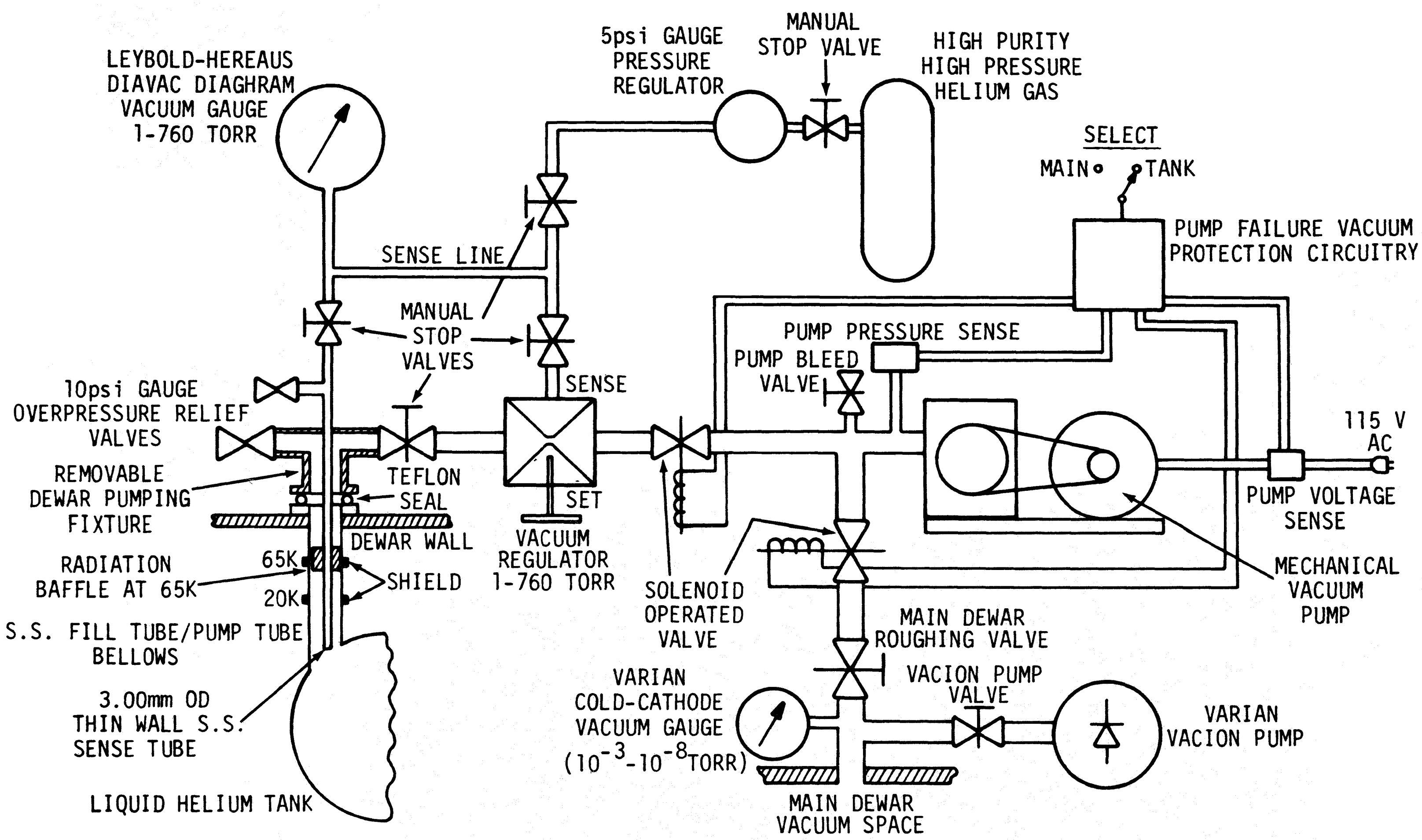

Fig. 8. The vacuum pumping and control system for the cryogenic dewar.

is readily achieved. Long term integrity of the dewar vacuum is assured, since the measured leak and outgassing rate after 24 hours of pumping with the Vac Ion pump is less than 10^{-7} std cc/sec for the complete assembly.

The helium tank may be evacuated via a special pumping fixture which attaches to the threaded fitting on the dewar flange and is sealed by a Teflon o-ring in a tapered seat. The Teflon o-ring is used because its sealing properties remain relatively unaffected by the cooling of the fixture produced by the cold outflowing helium gas. The pumping fixture has two separate ports - a main pump port and a vacuum sense line, which consists of a stainless steel tube which extends down the main dewar bellows tube to terminate at the joint between tank and tube. Soldered to the sense line, at the level of attachment of the bellows to the 65K shield, is a radiation baffle, cooled by gas conduction and radiation. The baffle is intended to significantly reduce radiation leakage down the pump tube to the helium bath. Overpressure relief valves (10 psi cracking pressure) are installed on both sense and pump ports to avoid catastrophic overpressurization of the helium tank. The main pump line is connected to the vacuum pump via a manually operated bellows sealed valve and a vacuum regulator, which can be used to control the vapor pressure of the helium gas in the tank and, hence, the bath temperature. The sense line is connected to a sensitive, mechanical diaphragm vacuum gauge and also to the sense port on the vacuum regulator, to enable precise control of the vapor pressure in the tank.

During initial start-up, the radiation shields will have been pre-cooled. The tank is usually filled with pure helium gas at about 1 atm at this stage and will remain substantially warmer (160K) than the 20K shield, because it is very weakly coupled to it. To further cool the tank, about 0.6 liter of liquid nitrogen is introduced, which reduces the temperature to about 80K in about 1 hour, before the liquid completely evaporates. When the liquid nitrogen is depleted, liquid helium is transferred from a storage dewar to complete the cooling to 4.2K and to fill the tank. The pump fixture is then installed and the vapor pressure in the tank lowered until the desired operating temperature is achieved.

V. Predicted and Measured Thermal Performance

Some important design parameters for the cryostat are summarized in Tables 1 and 2. Table 1 presents data on the total mass of the components at 2.5K, 20K and 65K and gives relevant data on the expected enthalpy change on cooling. For the 20K stage, with a 1020 refrigerator, the cooling times follow the approximate law $t = 0.5 + 0.34 * m$, where t is in hours and m is the total mass of copper attached to the stage in kg. Thus, the expected cooldown time for the 20K shield alone, in the absence of any external heat loads, would be about 4.8 hours. The measured times are i) 65K shield - 2.8 hours to 65K with $p < 10^{-5}$ torr; ii) 20K shield - a) 3.5 hours to 19.5K with helium tank removed, and b) 8.75 hours to 25K with helium tank installed and attaining a final temperature of 160K. The increased pre-cooling time for the 20K shield with the tank installed is due to radiative loading from the warmer tank to the colder shield.

To pre-cool the tank from 160K to 80K, using the latent heat of vaporization of liquid nitrogen only, should require, theoretically, 1.1 liter of liquid, although less than this is used in practice. To cool the tank and other associated components in a similar fashion from 80K to 4.2K with liquid helium, using only the latent heat of vaporization, should theoretically require the use of about 10 liters of liquid. As with the nitrogen, only about 7 liters is used in practice, indicating, in both cases that partial heat exchange with the cold gas evolved is aiding the cooling process. With a further 4.3 liters needed to fill the

TABLE 1

Estimated Total Mass of Material and Total Enthalpy Change

For Each of the Three Cryostat Stages

Stage	Estimated Mass/Material (kg)	Estimated Enthalpy Change (Joules)	
65K	13.6/copper	1.025×10^6	(300K - 65K)
20K	12.7/copper	1.00×10^6	(300K - 20K)
2.5K	8.8/copper	1.93×10^5	(160K - 80K)
		5.01×10^4	(80K - 4.2K)
		270	(4.2K - 2.5K)

TABLE 2

Estimated Heat Load on Each of the Three Cryostat Stages, Giving

A Breakdown by Heat Transfer Mechanism for Each Stage

Stage	Mechanism		Load (mW)	Total Per Stage (mW)
65K	Conduction:	Residual Gas Conduction ($P \sim 10^{-5}$ Torr)	186	
		3 fiberglass supports	4,000	
		Fill tube for tank	120	
		Heat strap for waveguides and coax	1,260	
	Radiation:	From 300K dewar wall	1,300	6,870
20K	Conduction:	Residual Gas Conduction ($P \sim 10^{-5}$ Torr)	34	
		3 fiberglass supports	320	
		Fill tube for tank	23	
		DC leads, waveguides and coax	134	
		Backshort mechanisms	300	
	Radiation:	Mainly from 300K to unshielded feeds	300	
	DC Power:	To FET amps	500	1,110
2.5K	Conduction:	4 fiberglass supports for tank	1.99	
		2 cold stage bracket support	5.96	
		Fill tube for tank	0.48	
		DC leads, IF lines and waveguides	2.00	
		Backshort drive couplings	1.60	
	Radiation:	From shield and down fill tube	1.50	13.53

tank, the total liquid consumption is 11.3 liters. Lowering the vapor pressure over the liquid to reduce the bath temperature to 2.5K will deplete the liquid contained in the tank since the bath and surrounding metal components are cooled using the latent heat of vaporization of the liquid helium. The enthalpy change of 4.3 liters of liquid helium between 4.2K and 2.5K is approximately 3.6 x 10^3 joules so that about 1.4 liters of liquid will be used to cool the liquid helium alone to 2.5K and a further 100 mL will be consumed in cooling the 8.8 kg mass of the copper tank and associated components. Thus, after cooling to 2.5K, about 2.8 liters of liquid should remain in the tank. The level cannot be directly measured in the present system with the pumping fixture in place.

Table 2 summarizes the source and magnitude of the thermal loads on the various stages of the cryostat. The estimated total thermal load on the 2.5K stage of 13.5 mW leads to an estimated hold time at this temperature of 150 hours, which is to be compared with the measured hold time of 128 hours. Considering the likely errors involved in the estimation of the total heat load, the initial volume of helium in the tank at 4.2K and the amount of liquid remaining in the tank after pumping down to 2.5K, the measured results are in reasonably good agreement with the predicted performance.

Long term temperature stability is excellent when the vacuum in the tank is controlled by the regulator with remote sense connection. Stabilities of better than $\pm$ 0.1K have been obtained over periods of several days with the cryostat operating at 2.5K. With a higher conductance vacuum system and higher capacity pump, operation below the lambda point (2.17K) would probably be possible. Because of the limited pumping capacity, the present system self limits at about the lambda point with the vacuum regulator wide open. Under these conditions, the hold time is reduced by about 40% to about 68 hours. No special precautions were taken in the design to restrict the pump tube circumference at the tank neck in order to reduce superfluid film flow, as operation at 2.5K is normally adequate to achieve good performance from SIS mixers incorporating lead alloy junctions.

VI. RF Performance

The mixers [6] and IF amplifiers [11] used in this receiver have been described extensively elsewhere. The synthesized solid-state LO system will also be described in another paper [13]. The junctions used in the mixers were fabricated by L. R. D'Addario to a NASA design [6] at NBS, Boulder, CO. Mixer performance with these junctions has not been as good as that obtained by Pan _et al._ [6]. The I-V characteristics of the devices tested are not as non-linear as those exhibited by the devices used by the NASA group. The junctions used here may also have significantly different capacitance to the earlier devices. Nevertheless, quite acceptable performance has been obtained with several two junction arrays with normal resistances of about 100 ohms at 2.5K. Figure 9 shows typical I-V responses for one of the junctions used in the receiver at various physical temperatures. Note that little improvement in sharpness of the current step is achieved by cooling below about 3K.

A precision, bias voltage supply is used to apply D.C. bias to each mixer in the receiver. The bias voltage can be manually adjusted over the range 0-100 mV or can be varied under computer control to facilitate computer-aided measurement and characterization of the SIS element. The bias is applied via a bias tee, shown schematically in Figure 5, which is integral with the mixer block. A four-wire connection is used to enhance the measurement accuracy through the long leads needed for thermal isolation in the cryogenic system. The bias

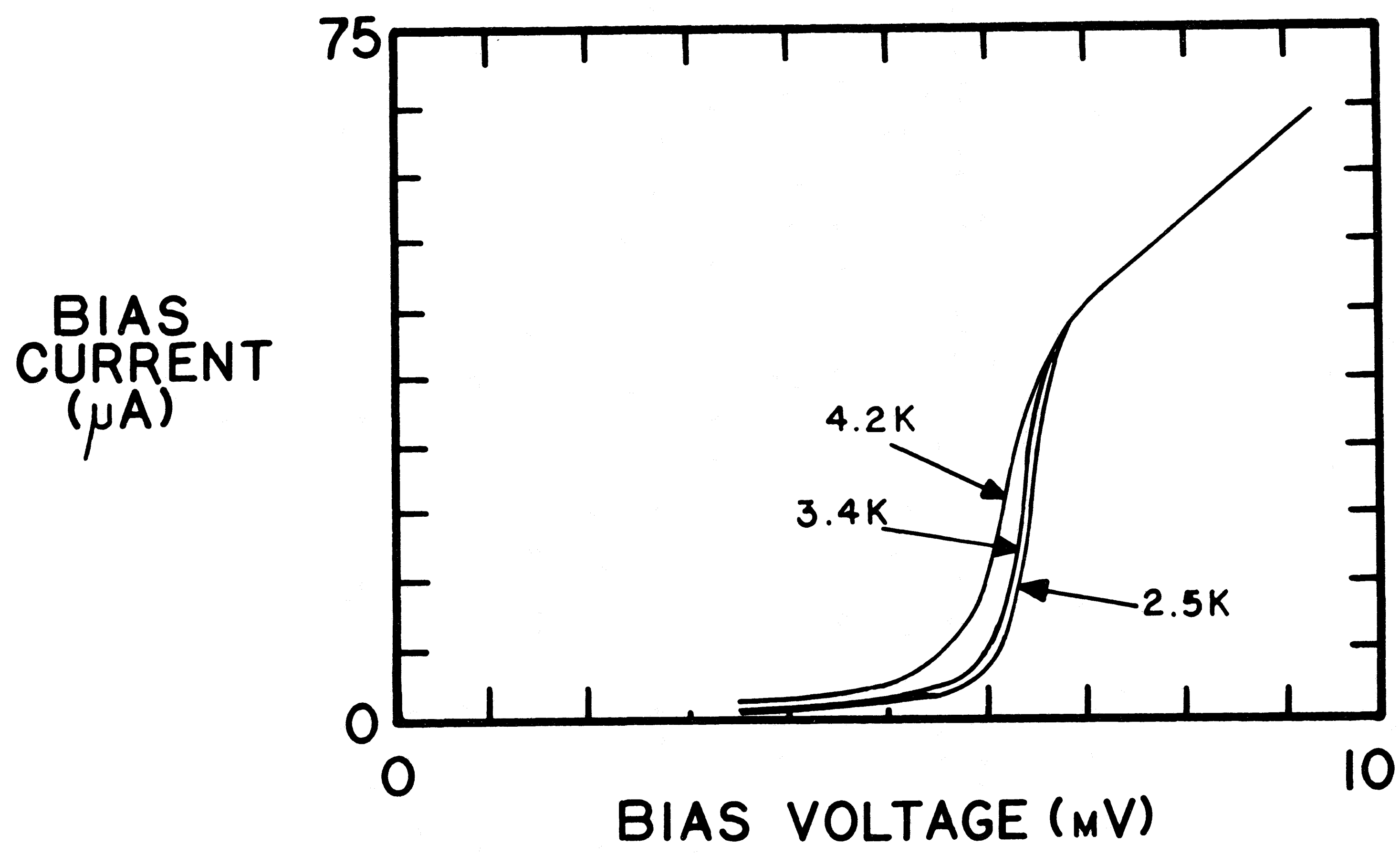

Fig. 9. The I-V response of the two-junction array of SIS junctions used in the mixer for which R.F. performance results are presented. The curves, measured at varying temperatures, show how the nonlinearity of the response can be enhanced by cooling the device to temperatures of 3K or below.

supply also includes a voltage sweep capability so that the junction I-V characteristic can be displayed on an x-y oscilloscope.

The current through the junction due to the applied L.O. signal is sensed and used to electronically control the L.O. power level so that the bias current in the mixer is held constant, as the backshort tuning is varied. L.O. power servoing is necessary for ease of mixer tuning, since the mixer reflection coefficient at the L.O. frequency can vary widely as the tuning of the relatively narrow band mixer is optimized.

A low power C.W. signal from an IMPATT sweep oscillator is injected along with the L.O. power, as shown in Figure 5. The IMPATT oscillator frequency can be rapidly switched between the upper and lower sidebands of the L.O. using a square wave modulating signal. The downconverted C.W. signals appearing at the I.F. output correspond to power converted from the upper and lower sidebands. By displaying the I.F. spectrum on a spectrum analyzer, the relative sideband gains can be estimated and the mixer tuning optimized for best single sideband operation.

Figures 10 and 11 show the performance of the two channel receiver. From Figure 10 it can be seen that the single sideband (SSB) receiver temperature in either channel is less than 120K between 100 and 120 GHz. The measured image rejection over this frequency range was > 15 dB. Figure 11 shows that the useable instantaneous receiver bandwidth at 110 GHz is at least 400 MHz in either channel. Table 3 gives an estimate of the loss and noise temperature budget for one channel of the receiver at 110 GHz.

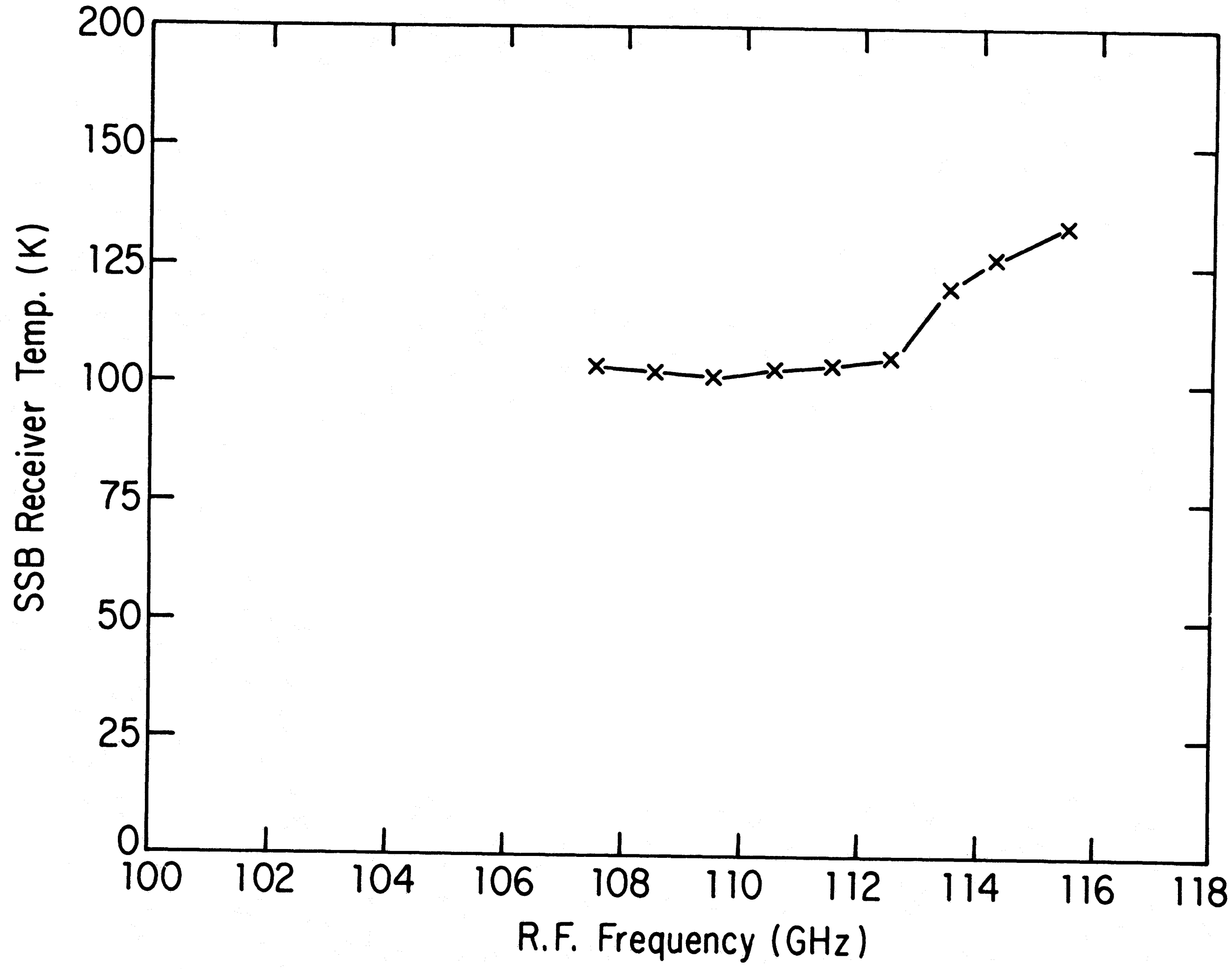

Fig. 10. The single sideband noise temperature of the complete receiver as a function of input frequency. The junction array with I-V curve shown in Figure 9 was used, cooled to 2.5K. The mixer tuning was adjusted to give an optimum response at the lower sideband of the local oscillator, with > 15 dB rejection of the upper sideband. The I.F. center frequency was 1.5 GHz with a 24 MHz instantaneous I.F. bandwidth. Mixed bias voltage was 5.6 mV at a current of 14 μA.

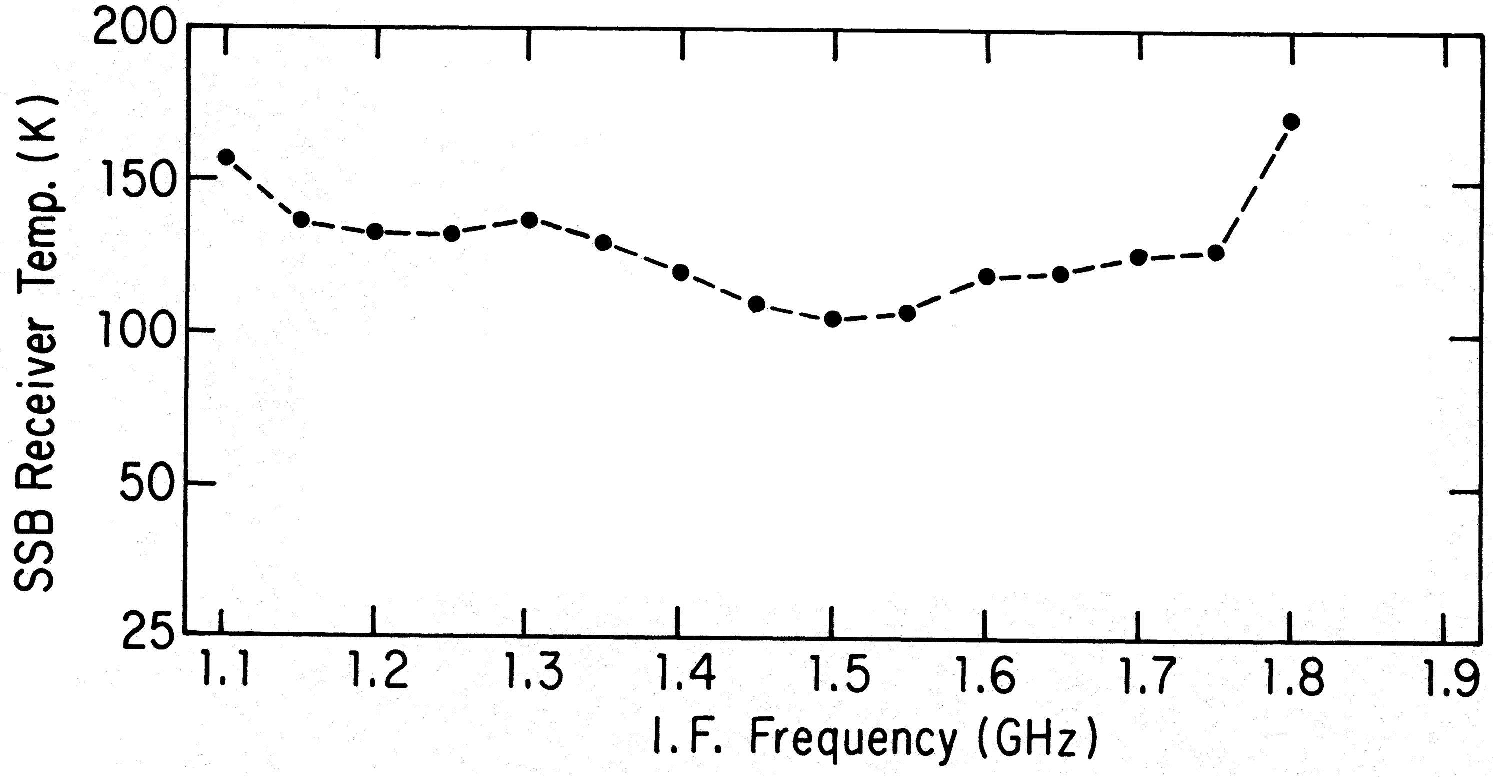

Fig. 11. The single sideband noise temperature of the receiver as a function of I.F. frequency at 110 GHz input frequency. Mixer physical temperature, tuning and bias conditions were the same as described for Figure 10. Again, the measurement I.F. bandwidth was 24 MHz.

TABLE 3

Estimated Loss and Noise Temperature Budget for One Channel

of the 100-120 GHz Receiver at 110 GHz

Component	(SSB) Gain (dB)	Physical Temperature (K)	Effective Noise Temperature (K)	Contribution to SSB Receiver Noise Temperature (K)
Polarization Diplexer	-0.05	300	3.30	3.30
Lens	-0.10	300	6.90	6.90
Feed Horn	-0.05	20	0.22	0.23
Gap Transition and Waveguides	-0.15	20	0.68	0.71
Crossguide Coupler	-0.30	2.5	0.17	0.18
SIS Mixer	-7.0	2.5	23.00	27.00
Isolator and Cables	-0.2	2.5	0.11	0.63
I.F. Amplifier	+30.0	20	10	60.95
TOTALS	+22.15			100

VII. Summary

This report has given a description of the construction and performance of a new design for a small hybrid liquid helium cryostat incorporating a dual polarized 100-120 GHz receiver. Very long helium hold times have been achieved at 2.5K, which will simplify maintenance of the receiver when it is installed on the NRAO 12-m radio telescope. The receiver noise performance is more than a factor of two better than NRAO's existing cooled Schottky diode mixer receiver and it is expected that the receiver temperature can be improved significantly when improved junctions become available.

VIII. Acknowledgements

The author wishes to thank M. Barkley, W. Luckado and G. Taylor for their excellent work in the fabrication of the receiver components. N. Horner, Jr. and R. Harris assembled the mixers and I. F. amplifiers, respectively. Thanks also go to L. R. D'Addario who fabricated the junctions used in the mixers and provided useful comments and suggestions.

REFERENCES

[1] J. W. Archer, Rev. of Sci. Instruments, vol. 54, no. 10, p. 1376 (1983).

[2] C. R. Predmore, N. R. Erickson, P. F. Goldsmith, J. L. R. Marrero, IEEE Trans. on MTT, vol. MTT-32, p. 498 (1984).

[3] G. J. Dolan, T. G. Phillips, and D. P. Woody, Appl. Phys. Lett., vol. 34, p. 347 (1979).

[4] P. L. Richards, T-M. Shen, R. E. Harris and F. L. Lloyd, Appl. Phys. Lett., vol. 34, p. 345 (1979).

[5] J. R. Tucker, IEEE Journal of Quantum Electronics, vol. QE-15, no. 11, p. 1234 (1979).

[6] S-K. Pan, M. J. Feldman, A. R. Kerr, and P. Timbie, App. Phys. Lett., vol. 43, p. 786 (1983).

[7] R. Blundell, J. Ibruegger, K. H. Gundlach and E. J. Blum, Elec. Lett., vol. 20, p. 476 (1984).

[8] E. C. Sutton, IEEE Trans. on MTT, vol. MTT-31, p. 589 (1983).

[9] L. R. D'Addario, to be published in Int. J. I.R. and MM Waves, vol. 5, no. 10, October 1984.

[10] R. C. Longsworth, Cryogenics, vol. 24, p. 175 (1984).

[11] S. Weinreb, D. Fenstermacher and R. Harris, IEEE Trans. on MTT, vol. MTT-30, no. 6, pp. 849-853 (1982).

[12] J. W. Archer and M. T. Faber, Int. J. I.R. and MM Waves, vol. 5, no. 8, p. 1069, August 1984.

[13] J. W. Archer, submitted to Rev. of Sci. Instruments, October 1984.

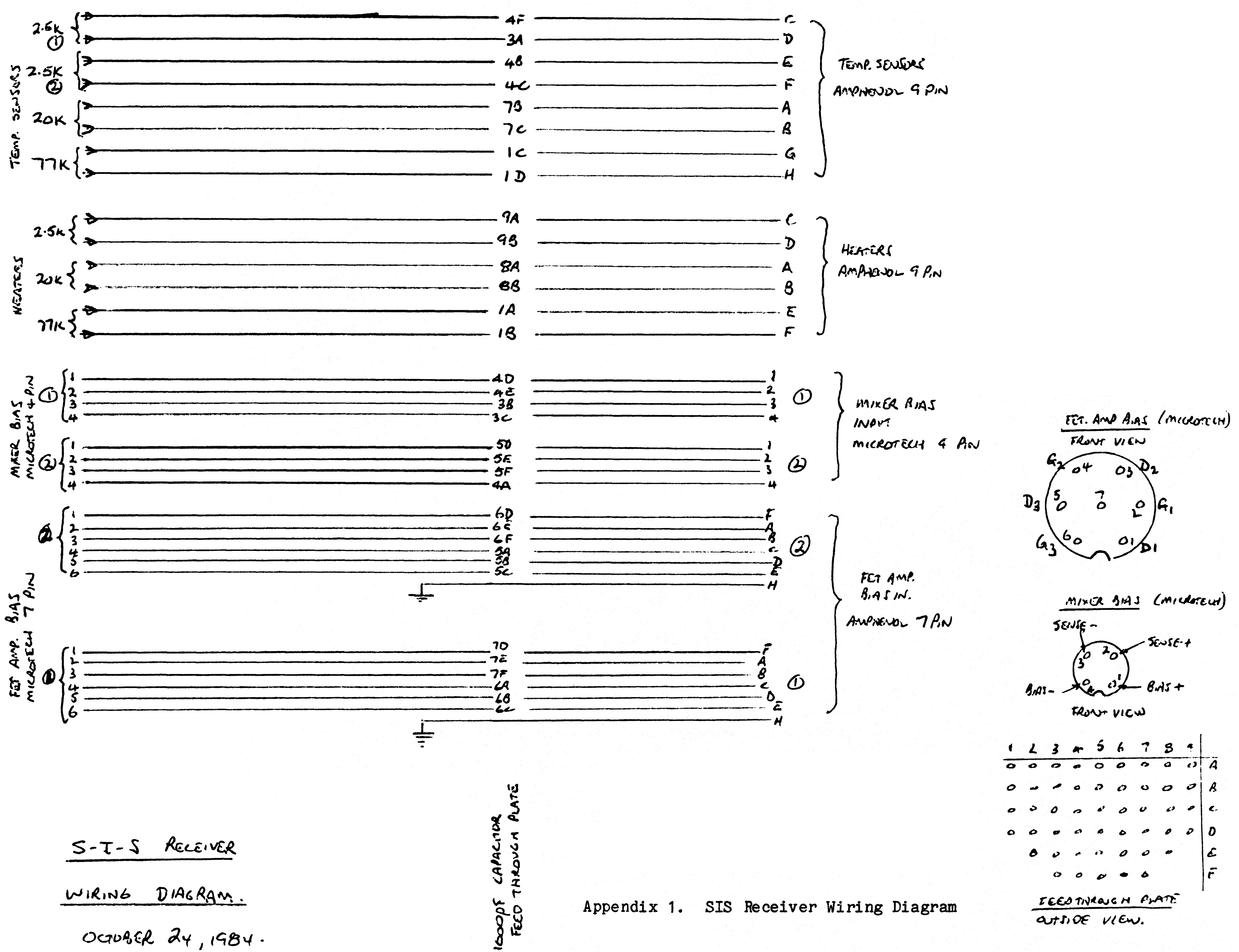

Appendix 1. SIS Receiver Wiring Diagram

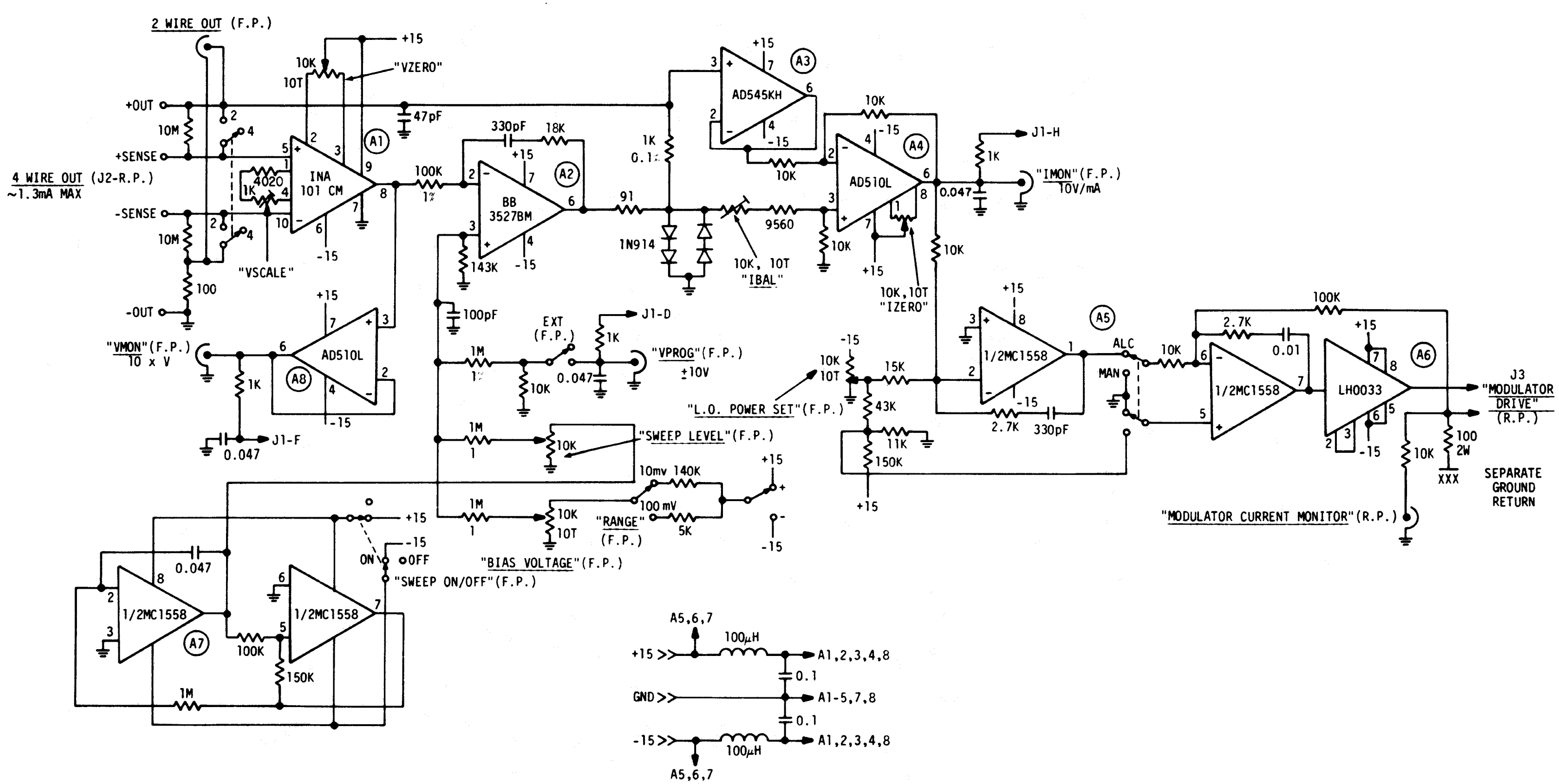

Appendix 2. SIS Receiver - Bias Supply for Mixer